Supporting information

Bi_2S_3 nanorods-stacked hollow microtubes self-assembled from bismuth-based metal–organic frameworks as advanced negative electrodes for hybrid supercapacitors

Xianbo Yu[a], Jiaojiao Zhou[a], Qin Li[a], Wen-Na Zhao[b,*], Shihang Zhao[a], Hongmei Chen[a], Kai Tao[a] and Lei Han[a,c,*]

[a] State Key Laboratory Base of Novel Functional Materials and Preparation Science, School of Materials Science & Chemical Engineering, Ningbo University, Ningbo 315211, China. E-mail: hanlei@nbu.edu.cn

[b] Key Laboratory for Molecular Design and Nutrition Engineering of Ningbo, Ningbo Institute of Technology, Zhejiang University, Ningbo, Zhejiang 315100,China. E-mail: wnzhao@nit.zju.edu.cn

[c] Key Laboratory of Photoelectric Materials and Devices of Zhejiang Province, Ningbo University, Ningbo, Zhejiang 315211, China.

Experimental section

Materials: Bismuth nitrate pentahydrate ($Bi(NO_3)_3·5H_2O$), Cobalt nitrate hexahydrate ($Co(NO_3)_2·6H_2O$), Nickel nitrate hexahydrate ($Ni(NO_3)_2·6H_2O$), hexamethylenetetramine (HMT)， methanol anhydrous (MeOH), 1,3,5-benzenetricarboxylic acid (H_3BTC), thiourea (CH_4N_2S) and ethanol. All reagents are commercially produced without further purification.

Synthesis of CAU-17 hexagonal prisms: The CAU-17 was preparation has been carried out

using the methods already reported and some modifications.[1,2] To a mixture of 1,3,5-benzenetricarboxylic acid (H_3BTC, 3.33 mmol) and ground $Bi(NO_3)_3 \cdot 5H_2O$ (0.31 mmol) uniformly add to 60 mL MeOH. Putting the mixture dissolved under ultrasonic. Then homogeneous solution transferring to a Teflon-lined stainless-steel autoclave and heated at 120 °C for 24 h. After cooling down to room temperature, the white powder were collected by filtration, and washed with MeOH. The final samples were dried at 60 °C for 3h.

Synthesis of hierarchical Bi_2S_3 microtubes: The obtained CAU-17 hexagonal prisms were added into 20 ml of an ethanol solution containing 100 mg of thiourea and magnetically stirred for 5 min at room temperature. Then, the reaction solution and heated to 160 °C for 6 h in 50mL Teflon-lined stainless-steel autoclave. After the reaction, black power of Bi_2S_3 was obtained, washed with deionized water and absolute ethanol for three times.

Synthesis of CoNi-LDH sheets: Typically, 2mmol $Co(NO_3)_2 \cdot 6H_2O$, 2mmol $Ni(NO_3)_2 \cdot 6H_2O$ and 8mmol hexamethylenetetramine (HMT) were dissolved in 30 mL distilled water under magnetic stirring to form solution, then the solution was transferred into 50 mL autoclave. The autoclave was sealed and maintained at 100 °C for 10 h, and then cooled naturally. Finally, the products were washed with H_2O and ethanol, then dried at 60 °C for 6 h.

Material characterizations: Powder X-ray diffraction (PXRD) patterns were implemented by a Bruker AXS D8 Advance diffractometer at 40 kV, 40 mA using a Cu Kα (1.5406 Å) at room temperature. The Fourier transformation infrared spectra (FTIR) the samples were recorded on a NICOLET-6700 infrared spectrometer in the range of 500–4000 cm^{-1} using the KBr pellet method. Scanning electron microscopy (SEM) images were obtained from Hitachi S-4800 a field emission

scanning electron microscope (FESEM) equipped with an energy dispersive spectrometer (EDS) and mapping operated at an acceleration voltage of 10.0 kV. Transmission electron microscope (TEM) images were recorded using a FEI Tecnai G2 F20 with an accelerating voltage of 200 KV. X-ray photoelectron spectroscopy (XPS) measurements were performed on a Thermo Scientific ESCALAB250-Xi. Nitrogen adsorption-desorption isotherms were measured at 77 K using ASAP 2020 analyzer. Thermogravimetric analysis (TG) curve was measured on SII TG/DTA 7300 instrument at a heating rate of 10℃/min.

Electrochemical measurements

The electrochemical performance of the tested electrodes was evaluated in a three-electrode system where a saturated calomel electrode (SCE) as the reference electrode and Pt wire counter electrode, respectively, which in a 1 M KOH aqueous solution by an electrochemical analyzer system, CHI660E (Chenhua, Shanghai, China). The working electrodes were fabricated from a mixture containing the Bi_2S_3 nanotubes (80 wt%), acetylene black(10 wt%), and polyvinylidene fluoride (PVDF) (10 wt%) with the 1-methyl-2-pyrrolidinone (NMP) to form a slurry. The slurry was then coated onto the nickel foam substrates (1.0 cm × 1.0 cm), and dried at 60 °C for over-night, after pressed at 10 MPa for approximately one minute. Cyclic voltammetry (CV), galvanostatic charge–discharge (GCD) and electrochemical impedance spectroscopy (EIS) are evaluation of electrochemical performance of working electrode.

The specific capacity (Qs, C g^{-1}) was calculated by the following equation:

$$Qs = \frac{I \times td}{m}$$

(1)

Where I is the current (A), td is the discharge time (s), m is the mass of electrode active materials (g).

Before assembling the hybrid supercapacitor, the two working electrodes with the mass loadings were optimized to be m^+/m^- ratios about 1:2, were soaked into 1 M KOH for 3 h. The energy density (E) and power density (P) were calculated on the basis of the total mass of the active materials of the two electrodes according to the following equations:

$$E = \frac{I \int V\, dt}{3.6m}$$

(2)

$$P = \frac{3600E}{\Delta t}$$

(3)

where I is the discharge current, V is the voltage window, t is the time for full discharge and m is the mass of working electrode for the assembled HSC devices.

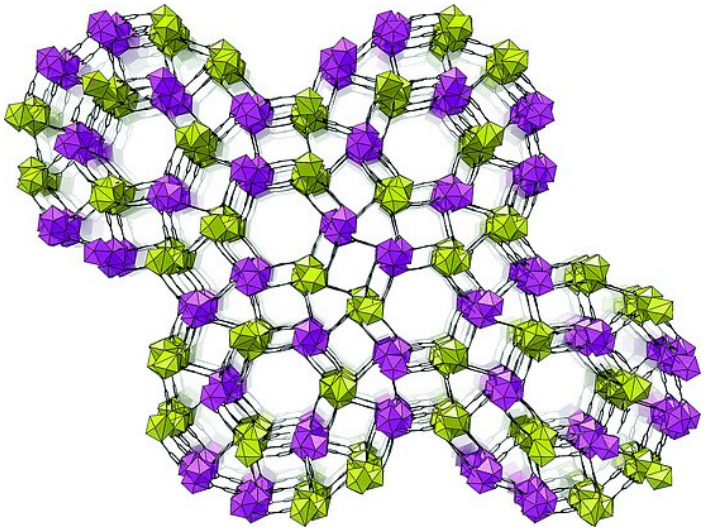

Figure S1. The structure of CAU-17.[2]

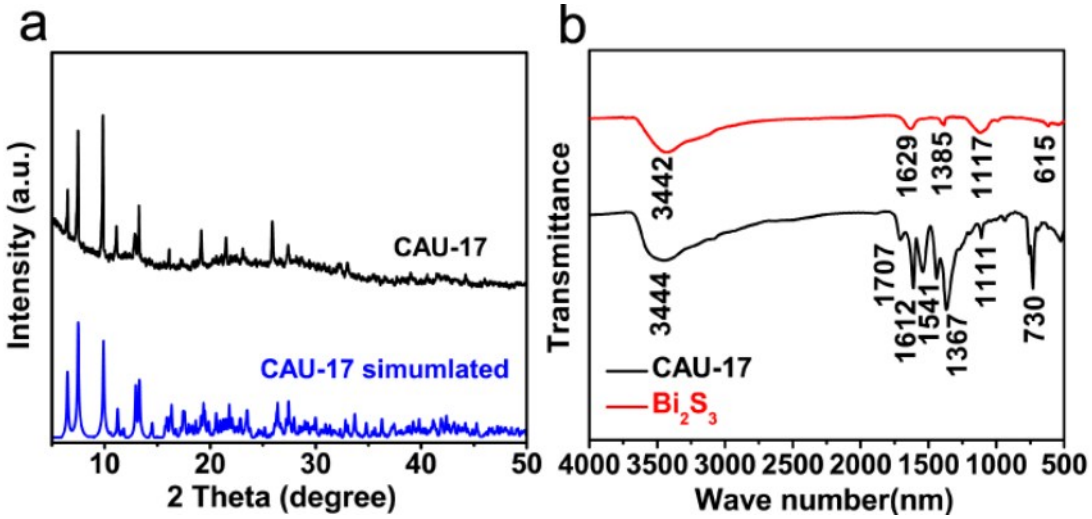

Figure S2. (a) XRD pattern of CAU-17 hexagonal prisms. (b) FTIR spectrum of CAU-17 and Bi_2S_3.

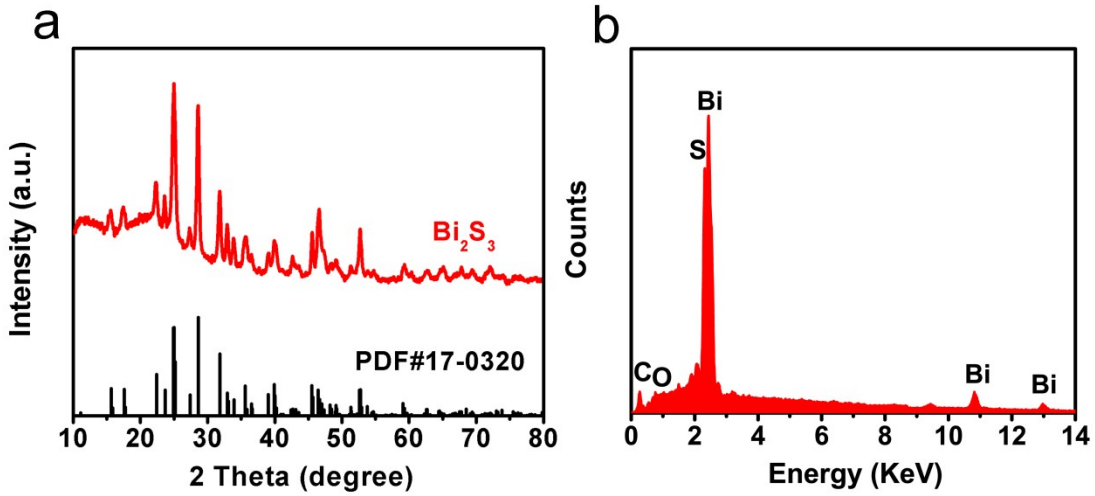

Figure S3. (a) XRD pattern of Bi_2S_3. (b) EDS spectrum of Bi_2S_3.

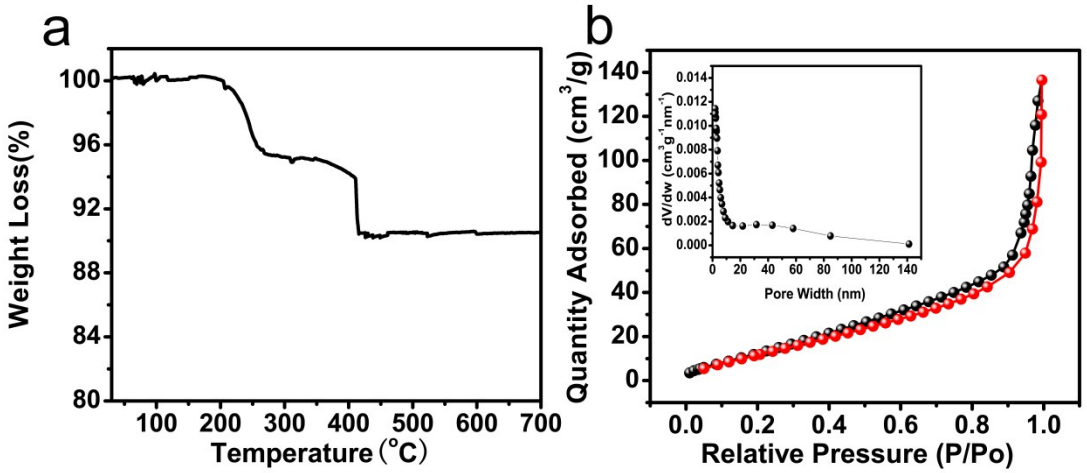

Figure S4. (a) TGA characterizations of Bi_2S_3. (b) N_2 adsorption/desorption isotherms of Bi_2S_3 and the pore size distribution of inset picture.

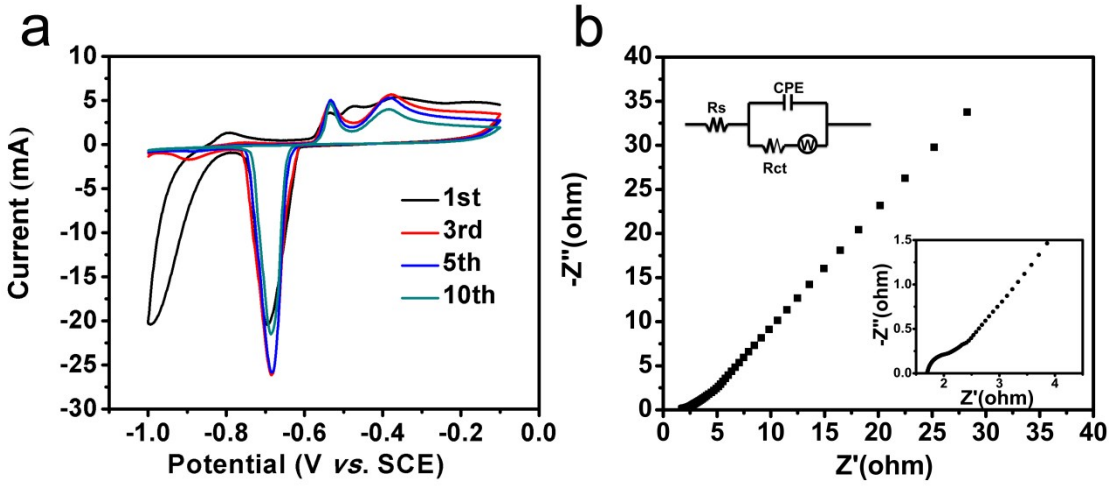

Figure S5. (a) The initial CV curves at a scanning rate of 5 mV s^{-1} at a scanning rate of 0.1 mV s^{-1}. (b) EIS

Nyquist plots of the Bi_2S_3 electrode and the inset shows the equivalent circuit.

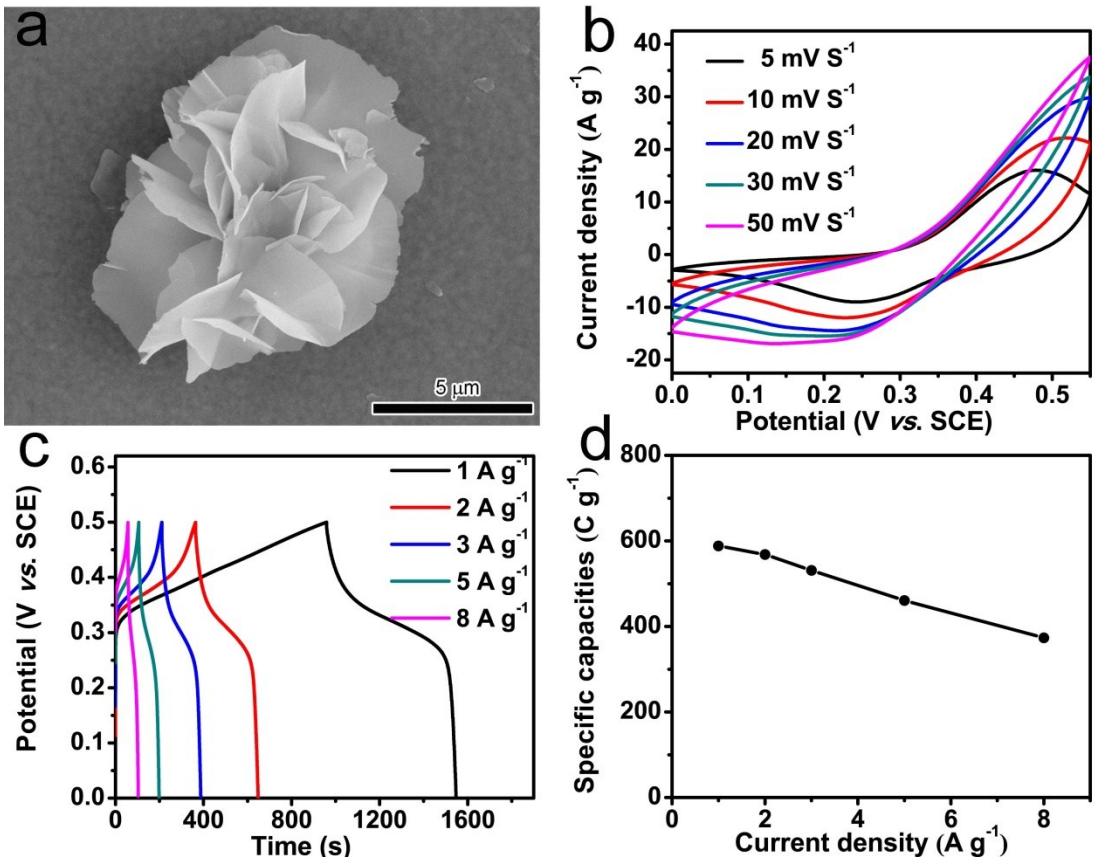

Figure S6. (a) SEM image of CoNi-LDH. (b) CV curves of CoNi-LDH electrode at different scan rates; (c) GCD curves of CoNi-LDH electrode at different current densities. (d) The specific capacity of CoNi-LDH.

Table S1. Electrochemical performance of representative bismuth based sulfide electrodes

Electrode materials	Specific capacities	Current density	Refs
Bi_2S_3	532 C g^{-1}	1 A g^{-1}	This work
Bi_2S_3	273 C g^{-1}	1 A g^{-1}	3
Bi_2S_3-rGO	238 C g^{-1}	1 A g^{-1}	4
Bi_2S_3-graphene	232 C g^{-1}	1 A g^{-1}	5
Bi_2S_3:PbS	242 C g^{-1}	1 A g^{-1}	6
Bi_2S_3	140 C g^{-1}	1mA/cm^2	7

References

1 H. Ouyang, N. Chen, G. Chang, X. Zhao, Y. Sun, S. Chen, H. Zhang and D. Yang, *Angew. Chem.,Int. Ed. Engl.*, 2018, **57**, 13197-13201.

2 A. K. Inge, M. Koppen, J. Su, M. Feyand, H. Xu, X. Zou, M. O'Keeffe and N. Stock, *J. Am. Chem. Soc.*, 2016, **138**, 1970-1976.

3 E. Miniach and G. Gryglewicz, *J. Mater. Sci.*, 2018, **53**, 16511-16523.

4 G. Nie, X. Lu, J. Lei, L. Yang and C. Wang, *Electrochim. Acta*, 2015, **154**, 24-30.

5 S. Vadivel, A. N. Naveen, V. P. Kamalakannan, P. Cao and N. Balasubramanian, *Appl. Surf. Sci.*, 2015, **351**, 635-645.

6 B. Pandit, G. K. Sharma and B. R. Sankapal, *J. Colloid Interface Sci.*, 2017, **505**, 1011-1017.

7 K. L. Liu, F. Chen, Y. Liu, D. Li and W. D. Shi, *CrystEngComm*, 2017, **19**, 570-575.